Chapter 4

Nanocrystalline Aggregation of Serine Detected by Electrospray Ionization Mass Spectrometry: Origin of the Stable Homochiral Gas Phase Serine Octamer

Portions published previously in: Julian R. R.; Hodyss R.; Kinnear B.; Jarrold M. F.; Beauchamp J. L. *J. Phys. Chem. B* **2002**, *106*, 1219-1228.

4.1 Introduction

Did homochirality precede life or was homochirality a consequence of life? This issue[1] is complex enough to warrant study from all avenues. This paper addresses a novel mechanism for the spontaneous generation of homochirality, or homochirogenesis. Homochirogenesis may be achieved by at least three fundamental mechanisms: 1) selective synthesis of only one enantiomer of a chiral molecule[2], 2) the preferential destruction of one enantiomer of a heterochiral mixture[3], and 3) separation of a racemic mixture into distinct homochiral parts.[4]

The spontaneous breaking of symmetry for a racemic mixture of chiral molecules has only been achieved by a handful of methods. Certain molecules will spontaneously separate from a racemic solution into homochiral crystals.[4] The assembly of these macroscopic homochiral crystals must be orchestrated at the molecular level.

Intermediate to the formation of macroscopic crystals from single molecules, noncovalently bound molecular clusters may be formed. The study of these intermediate molecular clusters is likely to offer insight into the most fundamental requirements for spontaneous symmetry breaking. Molecular clusters may share structural similarities with their parent crystal structures.[5] Furthermore, homochiral self-assembly into small molecular clusters offers a possible target of opportunity for conversion of the aggregates into a homochiral polymer or macromolecule with well-defined stereochemistry.

Electrospray ionization mass spectrometry (ESI-MS) is an excellent method for observing molecular clusters in the gas phase.[6] A variety of noncovalent clusters have been studied by ESI-MS, ranging from the molecular recognition of organic molecules[7] to the structures of salt clusters.[8] The flexibility and sensitivity of ESI-MS allows for the examination of solutions over a wide range of concentrations.

By itself, mass spectrometry provides only the molecular weight of a detected species and no direct information relating to molecular structure in general or to chirality in particular. This has led to the development of a variety of methods to circumvent this deficiency. These experiments, involving chiral amino acids[9], amino acid derivatives[10], tartrates[11], metals and amino acids[12], and host/guest chemistry involving crown ethers[13], cyclodextrins[14], cyclofructans[15], and monosaccharides[16] have all utilized mass spectrometry and taken advantage of the different physical properties of diastereomers to successfully discriminate between enantiomeric pairs. Experimental techniques include both kinetic and equilibrium methods. The preferred method uses one of the enantiomers isotopically labeled to distinguish it from the other.[8-16]

Alternatively, mass spectrometry can be coupled with another technique such as ion mobility spectrometry (IMS).[17] IMS gives direct structural information about the gas phase conformation of a molecule or cluster in the form of a collisional cross section. The experimental cross section can then be compared to the theoretical cross section determined computationally for likely structures of a particular molecule or cluster.

We have recently developed a new method to determine the extent to which spontaneous chiral separation occurs in small molecular clusters.[5,18] Our previous work[18] demonstrated the successful application of this new technique on the serine octamer. The serine octamer was originally reported by Cooks and coworkers,[19] using a different experimental methodology, to have a homochiral preference.

In the current work, we report detailed experiments that elucidate the structure of the serine octamer and offer an explanation for its unusual abundance. Examination of a mixture of D-serine and labeled L-serine using ESI-MS indicates that the octamer strongly prefers a homochiral composition. IMS experiments indicate that the structure of the octamer is consistent with a cubic arrangement of serine. Blockage of the N-terminus or C-terminus of serine leads to no octamer formation, suggesting that amino and carboxylate functionalities play a critical role in the bonding. The spontaneous symmetry breaking and likely involvement of zwitterionic serine aggregates in solution suggest that nanocrystals of serine precede the formation of the gas phase octamer. DFT calculations reveal several low energy structures that are related to the crystal structure of serine. The analogs threonine and homoserine may also form similar structures. The experimental results for these molecules are compared to the results found for serine.

4.2 Methods

Mass spectra were obtained using a Finnigan LCQ ion trap quadrupole mass spectrometer without modification. The signal was optimized using the automatic tuning capabilities of the LCQ on the protonated serine octamer. For serine and analogs, the settings used were source voltage 4.15 kV, capillary voltage 27.30 V, capillary temperature 159.9°C, and tube lens offset 10 V. Collision induced dissociation (CID) was performed on isolated parent ions by applying a resonance excitation RF voltage of between 0.98 V and 2.45 V for a period of 30 ms.

Sample concentrations were varied from ~10^{-5} to ~10^{-2} M for serine. The maximum octamer formation was observed at ~0.01 M. These concentrations are substantially higher than those used for analytical purposes. Samples were electrosprayed using a 50:50 methanol/water mixture containing 0.1% v/v acetic acid at a flow rate of 3 μL/min from a 500 μL Hamilton syringe. Silica tubing with an inner diameter of 12.7 microns was used as the electrospray tip. Unlabeled compounds were purchased from Sigma or Aldrich and used without further purification. L-serine labeled by replacing the hydrogen in the three C-H bonds with deuterium (99+ atom %, 98+% ee) was purchased from Cambridge Isotope and used without further purification.

Candidate structures were identified with molecular mechanics and submitted to full optimization at the PM3 level. All calculations at the PM3 semi-empirical level were performed using the HyperChem 5.1 Professional Suite. In Table 1, the structures were optimized at the PM3 level, followed by single point calculations at the DFT B3LYP/6-31G level, corrected for zero point energies. All remaining structures (i.e. those in Table 2) were fully optimized and analyzed utilizing DFT. These calculations were carried out

at the B3LYP/6-31G**//B3LYP/6-31G level and corrected for zero point energies using Jaguar 4.0 by Molecular Simulations, Inc. Cross sections for candidate structures were determined using a trajectory method with a Lennard-Jones potential.[20]

To determine the extent to which chiral separation occurs in molecular aggregates, a solution containing a mixture of enantiomers, with one labeled, is electrosprayed.[18] For each cluster, a distribution of peaks will be observed. For example, three peaks corresponding to the LL, LD(DL), and DD clusters will represent a dimer. If the structure of these noncovalently bound clusters is not sensitive to the chirality of the constituent molecules, then the relative intensities of the peaks will follow a binomial distribution. For the dimer above the predicted intensities would be LL=0.25, LD(DL)=0.5, and DD=0.25 for a mixture that was initially 50% of each monomer. If the stability of the cluster is sensitive to the chirality of the individual molecules, the observed distribution will deviate from the binomial distribution. A preference for homochirality will be indicated by an increase in the relative intensities of the pure L and pure D clusters. A preference for heterochirality might also be observed, with the mixed species being more abundant than predicted by the statistical distribution.

The experimental cross sections of the serine clusters were measured using a high-resolution ion mobility apparatus.[21] A solution was prepared by dissolving five milligrams of L-serine in 1 ml H_2O, 0.2 ml CH_3COOH, and 0.1 ml CH_3CN. The solution was electrosprayed using a 5 kV potential across a 0.5 cm gap. The ions were guided into a drift tube through an ion gate with a 556 Vcm^{-1} field against a 2000 sccm flow of helium. The 63 cm long drift tube contains 46 guard rings and was operated at 10,000 V with ~760 torr of helium buffer gas.

Ions exit the drift tube through a 0.125 mm aperture and are focused into a differentially pumped region where they are mass selected by a quadrupole mass spectrometer and detected by an off-axis collision dynode and dual microchannel plates. A multichannel scaler that is synchronized with an electrostatic shutter located between the ion gate and the drift tube records arrival-time distributions. Drift times are determined by correcting the arrival times for the time that the ions spend traveling from the drift tube to the detector. Collision cross sections are calculated using Equation 1.[22]

$$\Omega_{avg}^{(1,1)} = \frac{(18\pi)^2}{16}\left[\frac{1}{m}+\frac{1}{m_b}\right]^2 \frac{z_e}{\left(k_B T\right)^2}\frac{t_D E}{L}\frac{1}{\rho} \qquad (1)$$

In this expression, m and m_b are the masses of the ion and buffer gas, z_e is the charge on the ion, ρ is the buffer gas number density, L is the length of the drift tube, and E is the drift field. Ions with the same m/z but different structures have different collisional cross sections and can be distinguished.[23] This is particularly useful in distinguishing "multimers" where, for example, the peak for the singly charged monomer is overlapped by the doubly charged dimer.[24]

4.3 Results

Serine. Serine is the simplest amino acid with a polar side chain, the hydroxy-methyl group. The chiral center is marked with an asterisk in structure **4.1**. In separate ESI-MS experiments, the concentration of serine was varied by factors of ten from 10μM to 0.1M. Maximum clustering was observed at 0.01M concentration. The positive ion mass spectrum obtained with 0.01M L-serine is presented in Figure 4.1. The protonated octamer, $[8Ser+H]^+$, is the base peak in the spectrum, followed by an

abundant protonated dimer. It is interesting to note that all of the odd clusters, i.e. the trimer and pentamer, prior to the octamer are disfavored. All of the odd clusters after the octamer fit smoothly with the distribution of the even numbered clusters. Furthermore, at masses higher than the hexamer, there are abundant half-integer peaks corresponding to doubly charged clusters such as $[13Ser+2H]^{2+}$. At masses higher than the protonated 7mer (equivalent to the $[7Ser+H]^{+}$ notation), one-third-integer peaks arise corresponding to triply charged species such as $[23Ser+3H]^{3+}$. In general, the distribution of clusters with m/z higher than $[8Ser+H]^{+}$ exhibits greater relative intensities than those clusters with a lower m/z. Clearly, the most prominent feature of the spectrum is the unusual abundance of the protonated serine octamer.

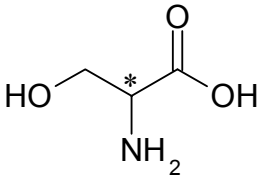

4.1

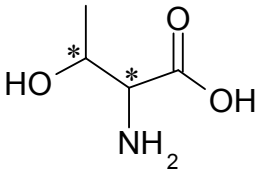

4.2

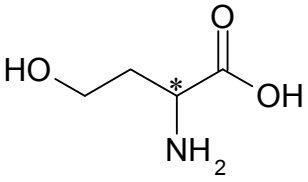

4.3

Ion mobility data (Figure 4.2) confirm that the peak corresponding to the serine octamer is itself comprised of three species, $[8Ser+H]^{+}$, $[16Ser+2H]^{2+}$, and $[24Ser+3H]^{3+}$. The relative intensities by peak height are 100, 75, and 28, respectively. The cross sections are 187 $Å^2$, 285 $Å^2$ and 380 $Å^2$, respectively. The theoretical cross section for a proposed structure should agree to within approximately ±2% of these numbers. This paper will focus on the structure of the octamer itself. In related studies, Clemmer and coworkers have discussed possible structures for the multimers and report a cross section of 191.4 $Å^2$ for $[8Ser+H]^{+}$.[25]

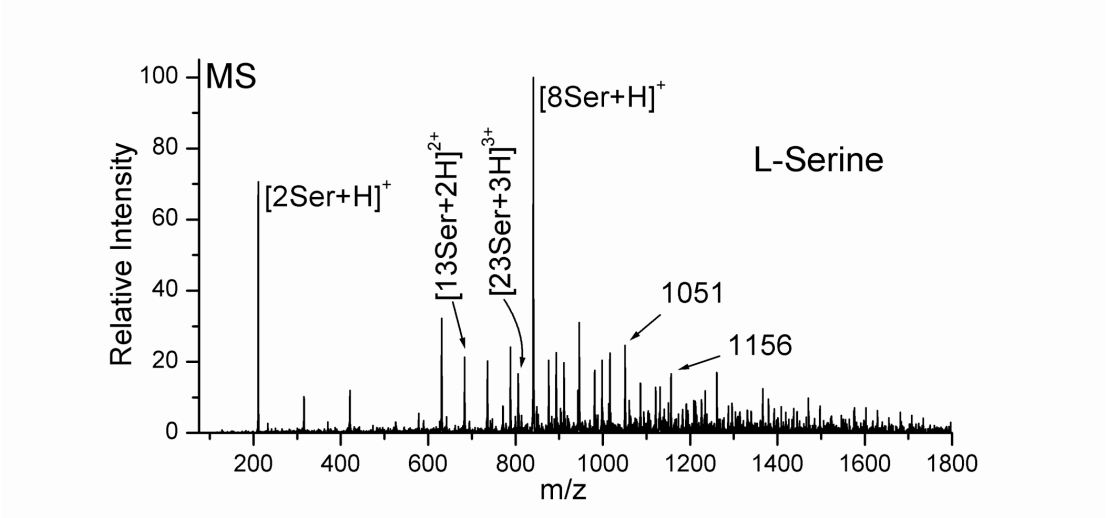

Figure 4.1 Mass spectrum of 0.01 M L-serine demonstrating abundant clustering and an unusually abundant octamer. Multiply charged as well as singly charged species are present.

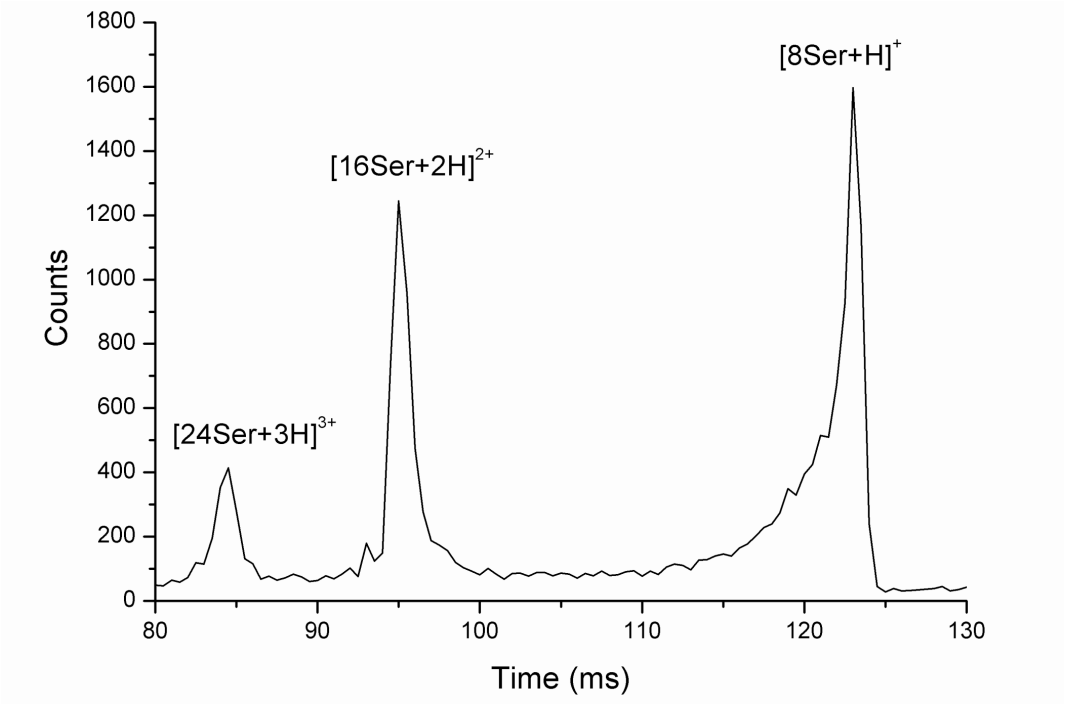

Figure 4.2 Ion mobility spectrum for m/z 841 from 0.036M serine. The three peaks correspond to the singly charged serine octamer and two multiply charged multimers.

The spectrum for the collision induced dissociation (CID) of the isolated singly protonated octamer is presented in Figure 4.3a. In the ion trap, the process of isolating ions with a certain m/z often leads to collisional heating with the helium bath gas. In this case, collisional heating eliminated all of the multiply charged serine clusters as evidenced by ^{13}C distribution. The most abundant fragment corresponds to the loss of two neutral serines, leaving the singly protonated hexamer. To a lesser extent, the singly protonated pentamer and tetramer are formed. The virtual absence of the heptamer is noted, suggesting that the loss of a single neutral serine is not favored.

The CID spectra for two of the higher mass clusters are presented in Figures 4.3b and 3c. The dissociation of the peak at m/z 1051 yields almost exclusively peaks separated by 35 mass units (Figure 4.3b). This corresponds to 1/3 the mass of serine, suggesting that the peak at 1051 is primarily composed of $[30Ser+3H]^{3+}$. In Figure 4.3c similar behavior is noted for the CID of the peak at m/z 1156. However, in this case there is an additional series of peaks separated by 35 mass units with m/z ratios higher than 1156. This series could only have resulted from a larger cluster with more than three charges on it, most likely $[44Ser+4H]^{4+}$. The relative intensities of the two series indicate that the quadruply charged species comprises a significant portion of the total intensity for the peak at m/z 1156.

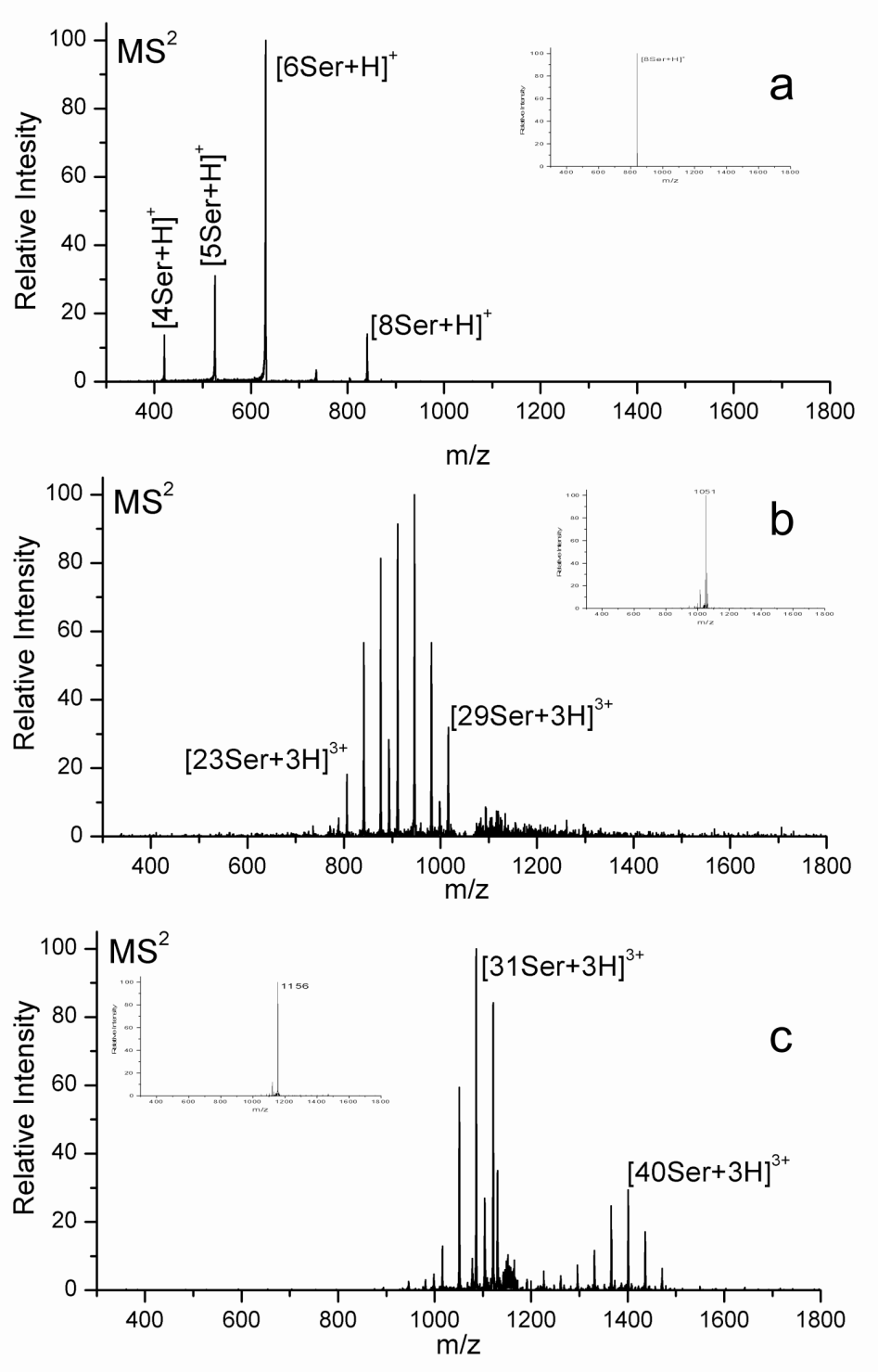

Figure 4.3 (a) CID spectrum for the singly charged serine octamer. The octamer preferentially loses a neutral serine dimer. (b) CID spectrum for m/z 1051. Several fragments are separated by 35 m/z, indicating that the parent ion is composed primarily

of $[30Ser+3H]^{3+}$. (c) CID spectrum for m/z 1156. The emergence of a cluster distribution with a separation of 35 m/z at a higher m/z suggests that a significant portion of this cluster is composed of $[44Ser+4H]^{4+}$.

Figure 4.4a shows the distribution of serine octamer clusters observed in a 54:46 mixture of D-serine with L-serine, respectively. The L-serine is labeled with deuterium in the three C-H bonds. In these experiments, collisional heating of all ions by mild excitation of the entire mass range was used to eliminate the multiply charged clusters, yielding only singly charged octamer peaks. The resulting experimental distribution of mixed clusters differs significantly from the predicted statistical distribution, included in Figure 4.4a for comparison. These results are in stark contrast to those for the serine dimer. Figure 4.4b illustrates the results of the same experiment for the protonated serine dimer in which no preference for homochirality is observed.

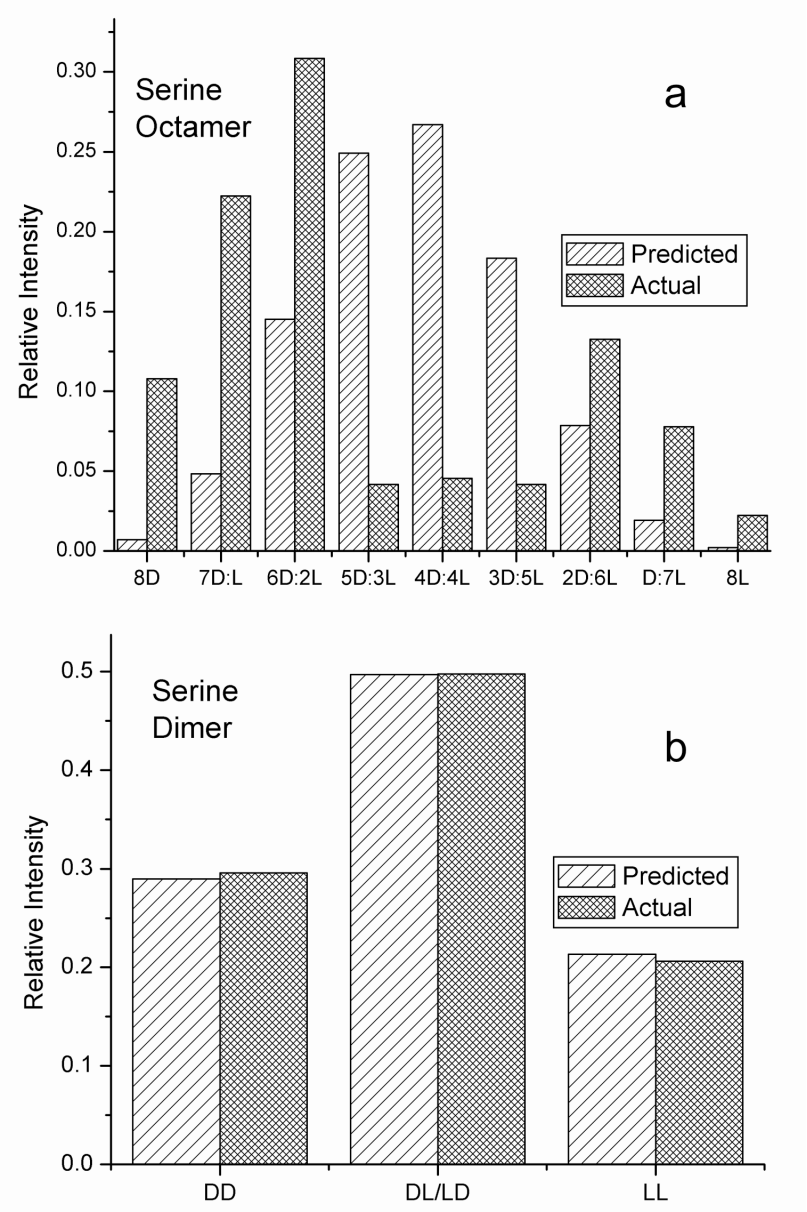

Figure 4.4 (a) Comparison between the predicted statistical distribution and observed distribution for the serine octamer for a 54:46 mixture of D-serine and isotopically labeled L-serine. Full spectrum CID was used to break up the multiply charged aggregates of the octamer. A clear preference for homochirality is indicated by this data. (b) Comparison between the predicted statistical distribution and observed distribution for the serine dimer. No clear preference for chirality is indicated.

At first glance the data in Figure 4.4a suggests that octamers containing a mixture of 6D and 2L or 2D and 6L serines are favored. A more detailed analysis is shown in Figure 4.5. Dividing the observed intensities by the statistical prediction (Figure 4.5a) yields relative intensities for the octamers which better reflect their energetic stabilities. This is more evident in the semilog plots in Figures 4.5b and 4.5c, where starting with either the 8D or 8L octamers, respectively; there is a sequential replacement of serines of one enantiomer with the other. In both instances the limiting case of a single replacement indicates an energetic cost of 2.9 ±0.3 kJ/mol, calculated from the slope of the semilog plot assuming a Boltzmann analysis is valid, for incorporating the incorrect enantiomer in the homochiral cluster.

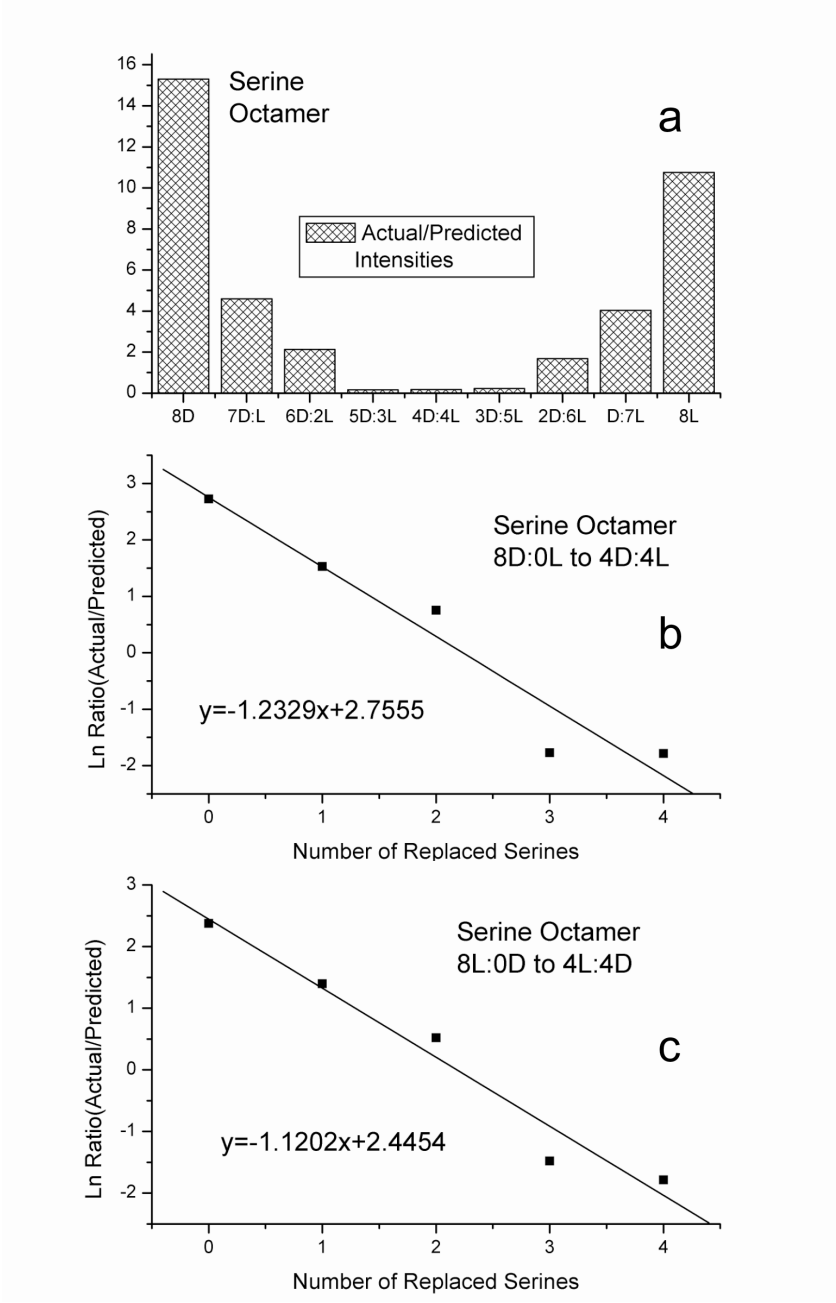

Figure 4.5 (a) Ratio of the observed to statistical intensities for the serine cluster distribution shown in Figure 4a. (b) Plot of the ln of the ratios in (a) versus the number of L-serines switched for D-serine starting with the D-serine octamer. (c) Plot of the ln of the ratios in (a) versus the number of D-serines switched for L-serine starting with the homochiral L-serine octamer.

Serine Derivatives. The spectra for L-serine methyl ester and L-N-tertbutoxycarbonyl-serine (L-tboc serine) are shown in Figures 4.6a and 4.6b, respectively. As seen in Figure 4.6a, the C-terminal methyl ester group eliminates the pattern of clustering that is observed for serine. The dimer is the only prominent peak in the spectrum. The small distribution of clusters at higher masses contains multiply charged clusters of L-serine methyl ester with sodium (present as a contaminant). Similarly in Figure 4.6b, the dimer of L-tboc serine is the dominant peak, followed by some higher order clusters. The trimer and higher mass clusters are primarily sodiated. The distribution of clusters is again quite different than that observed for serine itself (Figure 4.1).

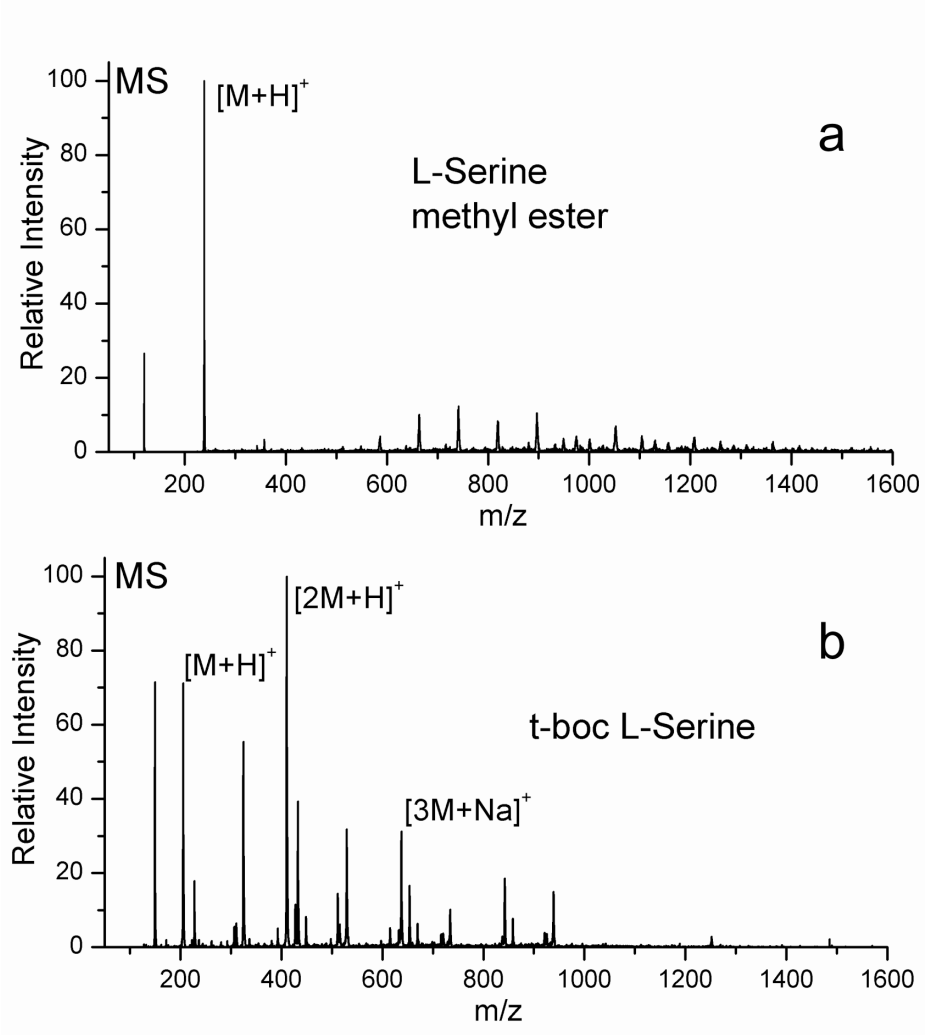

Figure 4.6 (a) Mass spectrum of L-serine methyl ester. There is no evidence for an unusually abundant octamer. (b) Mass spectrum of t-boc serine. Again, there is no evidence for an unusually abundant octamer.

Homoserine and Threonine. Two amino acids closely related to serine are threonine (structure **4.2**) and homoserine (structure **4.3**). Homoserine contains an additional methylene group, which extends the side chain relative to serine. The mass spectrum for L-homoserine is presented in Figure 4.7a. The monomer and dimer are both abundant, but the singly charged octamer does not exhibit unusual abundance (in contrast with serine). The base peak corresponds to 477 m/z, which might suggest that homoserine forms an unusually abundant tetramer. However upon closer inspection of the carbon-13 peaks, it becomes clear that the peak at 447 m/z is primarily composed of $[8Hser+2H]^{2+}$ (where Hser = L-homoserine). Therefore, homoserine also forms an unusually abundant octamer. The peak corresponding to $[11Hser+2H]^{2+}$ is also unusually abundant with respect to the surrounding distribution.

Several experiments were performed with mixtures of L-homoserine and L-serine. A 50/50 mixture of L-serine and L-homoserine will yield mixed clusters, but the mixed clusters are not unusually abudant. A 6/2 mixture of L-serine/L-homoserine yields abundant mixed serine octamers with the incorporation of 1 or 2 homoserine molecules into the cluster (Figure 4.7b). Isolation of $[6Ser+2Hser+H]^{+}$, followed by CID yields the spectrum shown in Figure 4.7c. The mixed cluster preferentially loses two neutral serines. Homoserine is always retained.

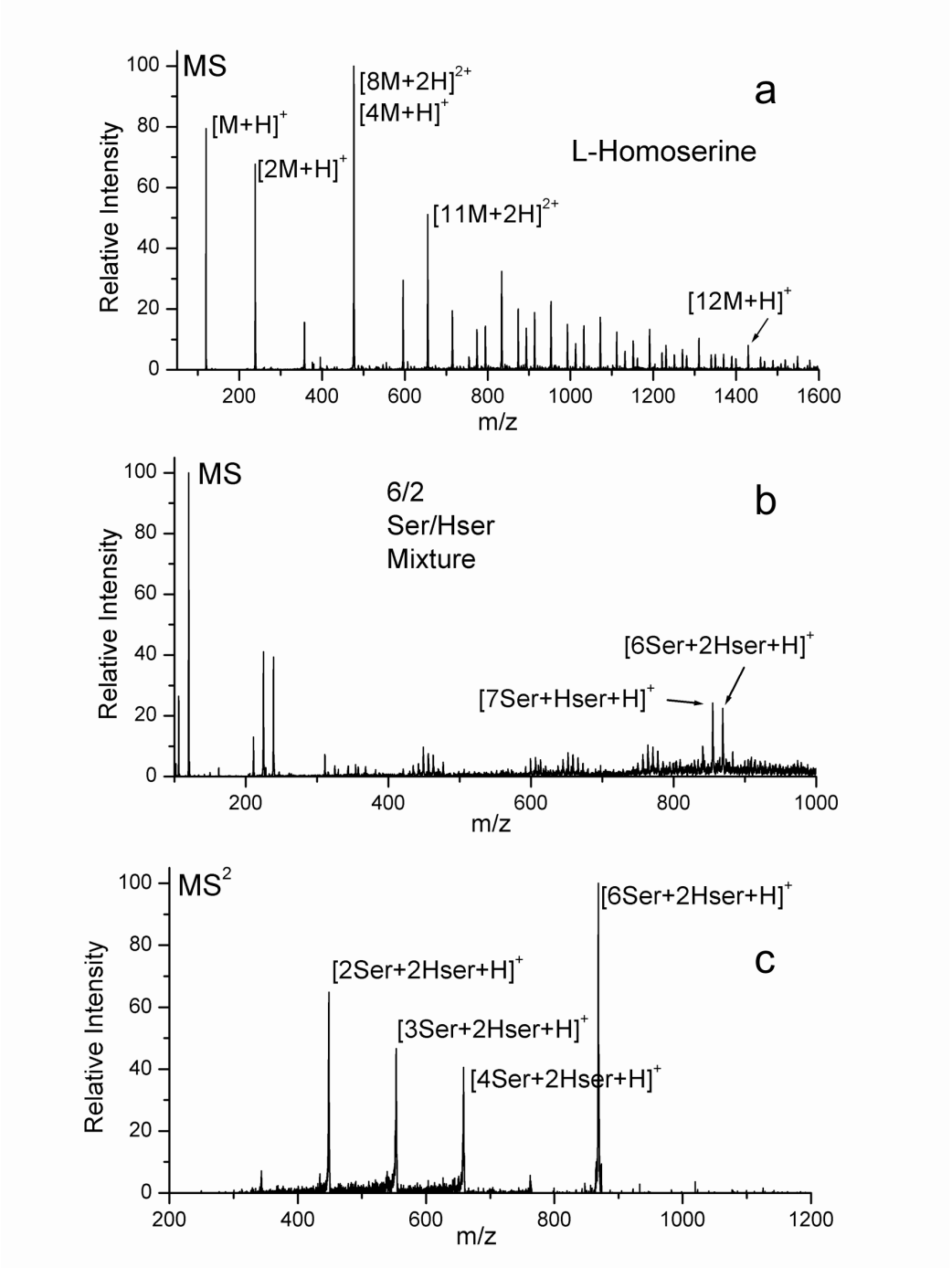

Figure 4.7 (a) Mass spectrum of L-homoserine showing extensive clustering and an abundant octamer. (b) Spectrum for a 6:2 mixture of serine and homoserine. (c) Collision induced dissociation on the mixed octamer yields the loss of at least two serines. Homoserine is always retained.

The mass spectrum for D-threonine is shown in Figure 4.8 (allo-threonine isomers gave very similar results). This spectrum shares many similarities with the spectrum of homoserine. As in the case with homoserine, $[8Thr+H]^{+}$ and $[8Thr+2H]^{2+}$ are both present. $[7Thr+H]^{+}$ is only prominent in the threonine spectrum. The peak corresponding to $[11Thr+2H]^{2+}$ is unusually abundant. However, the combined intensity of the octameric peaks is not as prominent as it is in the case of serine or homoserine.

A 50/50 mixture of D-threonine and D-serine was electrosprayed and is shown in Figure 4.9a. The singly and doubly charged mixed octamers are labeled in Figure 4.9a, where it is observed that they exhibit unusual abundance when compared to the other clusters. Figure 4.9b shows the distribution for the singly charged mixed threonine/serine octamer. Mixed clusters ranging from $[6Ser+2Thr+H]^{+}$ to $[2Ser+6Thr+H]^{+}$ are easily observed. The abundance of the two remaining mixed clusters and the two pure clusters cannot be discerned from noise. A similar distribution is observed for the doubly charged mixed octamers ($[6Ser+2Thr+2H]^{2+}$ to $[2Ser+6Thr+2H]^{2+}$) in Figure 4.9c. The different distribution, particularly the extra prominence of $[4Ser+4Thr+2H]^{2+}$, is likely due to the overlap with mixed tetramers such as $[2Ser+2Thr+H]^{+}$.

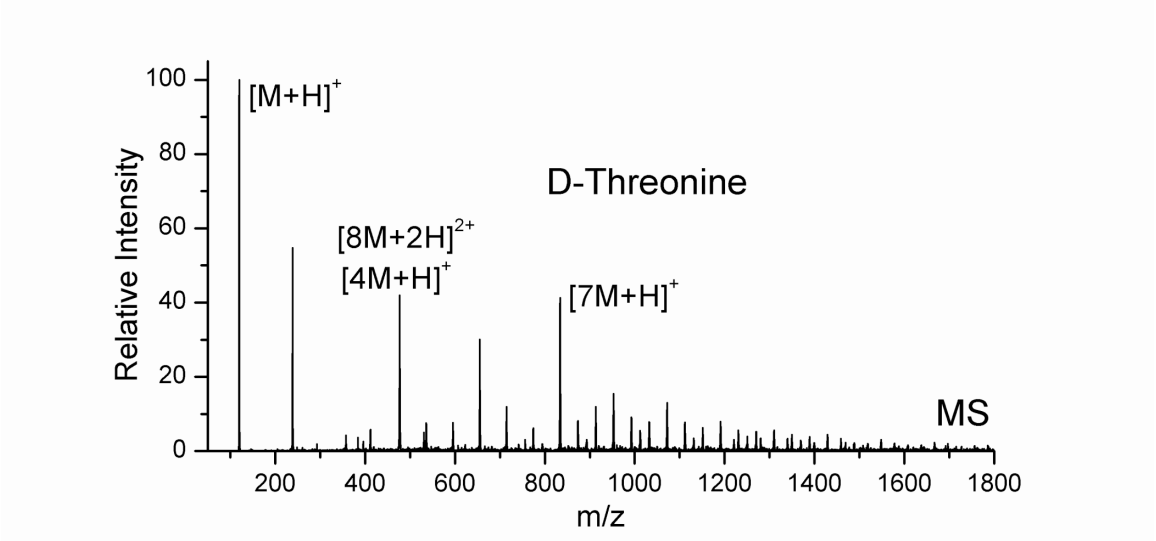

Figure 4.8 Mass spectrum for D-threonine. The octamer of this species is primarily doubly charged.

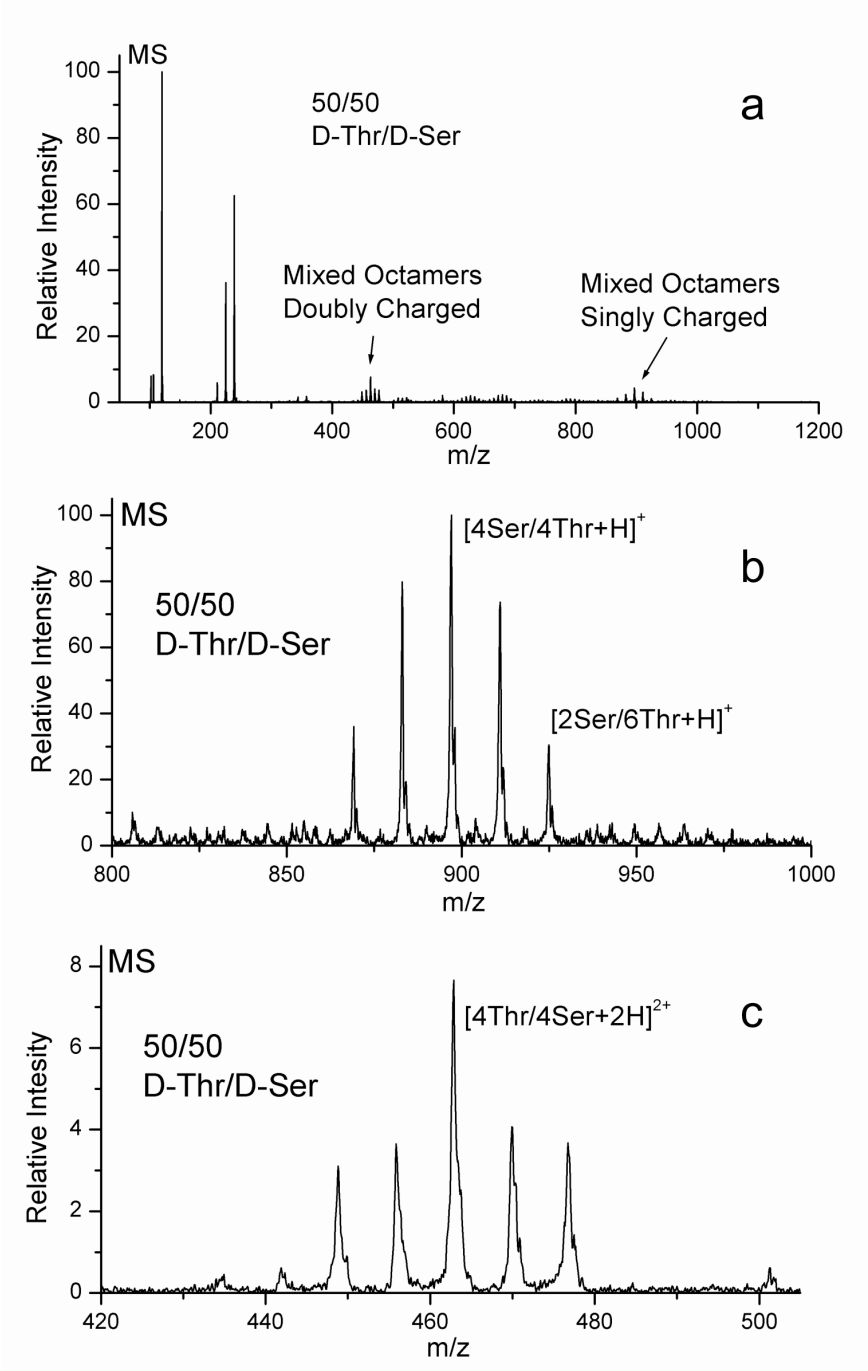

Figure 4.9 (a) Mass spectrum for a 50:50 mixture of D-threonine with D-serine. The mixed clusters still form octamers with unusual abundance. (b) Mass spectrum for the singly charged mixed octamers. (c) Mass spectrum for the doubly charged mixed octamers.

4.4 Discussion

The experiments presented thus far place several constraints on the structure of the serine octamer. (1) The unusual abundance of the octamer suggests a very stable structure. (2) The ESI-MS experiments in Figure 4.4 suggest that the octamer must have strong preference for homochirality. (3) Ion mobility data is consistent with a single structure with a cross section of 187 $Å^2$. (4) Figures 4.9b and 4.9c suggest that the structure should allow for the mixing of serine and threonine to give a stable octamer. Any structure that is proposed for $[8Ser+H]^+$ must be consistent with and account for these results.

Fundamentally, crystal formation begins in solution when molecules assemble themselves in a highly ordered fashion. This molecular organization is selective, and can lead to spontaneous symmetry breaking.[4] The serine octamer demonstrates selectivity which leads to homochiral molecular clusters. Might the homochiral preference of the serine octamer be derived from solution aggregates that are precursors to the formation of crystalline serine?

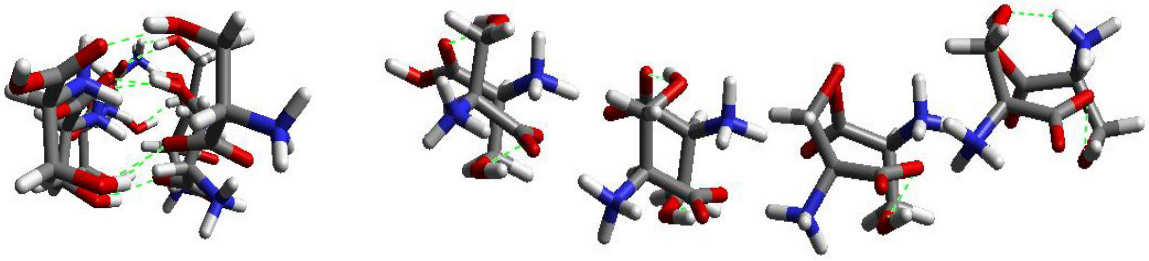

4.4

Crystalline L-serine is bound through zwitterionic salt bridges and by rows of hydrogen bonds between the hydroxy-methyl side chains.[26] Structure **4.4** is derived from the crystal structure of L-serine, where four of the hydroxy-methyl groups have been

rotated by ~120° relative to the crystal structure. The resulting structure has two rows of salt-bridges formed by zwitterionic serine in addition to hydrogen bonding between each hydroxy-methyl side chain and the carboxylate group of the serine in the opposite row. The minimized protonated gas phase structure as determined by DFT opitimization is shown in **4.4**. The addition of a proton causes the structure to curl relative to the more linear neutral structure.

Structure **4.4** is formed from zwitterionic serine, which is the predominant form of serine in both solution and the solid phase. Would a zwitterionic structure also be stable in the gas phase? Table 4.1 demonstrates the progressive stabilization of zwitterionic serine with increased cluster size for a model structure similar to **4.4**, in the absence of any net charge. The structures are stabilized in the zwitterionic state by the coulombic attraction that is derived from the two rows of salt bridges. This coulombic attraction compensates for the energy required to generate zwitterionic serine, which is not the lowest energy structure for the isolated serine molecule in the gas phase. If the coulombic attraction overcomes the "zwitterion penalty," the zwitterionic state of the cluster will be favored. A net charge has been shown previously to enhance the stability of zwitterions in the gas phase.[27] Our calculations indicate that structures similar to **4.4**, with varying numbers of serines in the chain, would be stable as zwitterions with eight or more serine molecules, even with errors of 5-10 kcal/mol in the calculations.

Table 4.1 Progressive Stabilization of Structure 4.4 at Various Chain Lengths.

Structure	Zwitterion[a] (kcal/mol)	Neutral[a] (kcal/mol)	Δ (kcal/mol)	Δ/Ser (kcal/mol)
2mer	-500335	-500342	7	3.5
4mer	-1000716	-1000726	10	2.5
6mer	-1501103	-1501094	-10	-1.6
8mer	-2001491	-2001468	-23	-2.9
10mer	-2501870	-2501825	-45	-5.7

a.) Total energy as determined by single point calculations on the PM3 minimized neutral structures at the 6-31G//B3LYP level, corrected for zero point energies.

Thus **4.4** is a reasonable candidate structure for the serine octamer because it can exist both in solution and the gas phase. Furthermore, **4.4** is a derivative of the crystal structure of L-serine, and as a result displays a strong preference for homochirality. It is not possible to change the chirality of four of the serines and generate a cluster composed of 4 D-serines with 4 L-serines (a 4D/4L cluster). The highly ordered bonds of **4.4** suggest that the structure may be very stable. This is confirmed in Table 4.2, which lists the calculated gas phase cross sections with the accompanying solution and gas phase energetics of several possible structures for the serine octamer. In solution, **4.4** has the best binding energy of the three structures. However, the calculated cross section for the protonated structure is 224 $Å^2$, which is much greater that the experimental value of 187 $Å^2$. Therefore **4.4** must be ruled out as the *gas phase* structure for the serine octamer.

Structure **4.5** is a cubic arrangement of eight serines that is closely related to **4.4**. Structure **4.5** is formed by taking **4.4** and essentially folding it in half to form a cube like structure. The structure has four rows of salt bridges, two interior and two exterior. The structure shown is the minimized unprotonated structure. The cross section calculated for

the neutral structure **4.5** is in reasonable agreement with the experimental results (Table 4.2). However, structure **4.5** undergoes significant reorganization in the gas phase when protonated. The protonated structure will not properly minimize, suggesting that it is significantly unstable in the gas phase. Furthermore, the two interior rows of zwitterions are not well exposed, leading to unfavorable solvation energetics which substantially decrease the solution phase binding energy (Table 4.2). Additionally, a similar heterochiral 4D/4L structure exists. Therefore, it is unlikely that **4.5** is the structure for the serine octamer, but it may be an important intermediate structure as will be explained below.

Table 4.2 Calculated Energetics and Cross Sections for Structures 4-6.

Structure	Relative Gas Phase Energy (kcal/mol)[a]	Computed Cross Section (Å^2)	Relative Gas Phase Binding Energy (kcal/mol) [a ,d]	Relative Solution Phase Binding Energy (kcal/mol)[e]
4	76	224 [b]	112	-55
5	--[f]	196 [c]	--	-16
6	0	189 [b]	0	0

a) Energies listed relative to **6** for protonated octamers

b) Cross sections for protonated structures to be compared with an experimental value of 187 Å^2

c) Cross section calculated for neutral structure (the neutral cross sections for **4.4** and **4.6** are 227 and 189 Å^2, respectively)

d) Binding energy calculated relative to eight separated zwitterionic serines

e) Energies calculated for neutral octamers in water with a dielectric constant of 80.37 and a probe radius of 1.4

f) This structure is not well behaved and does not fully minimize.

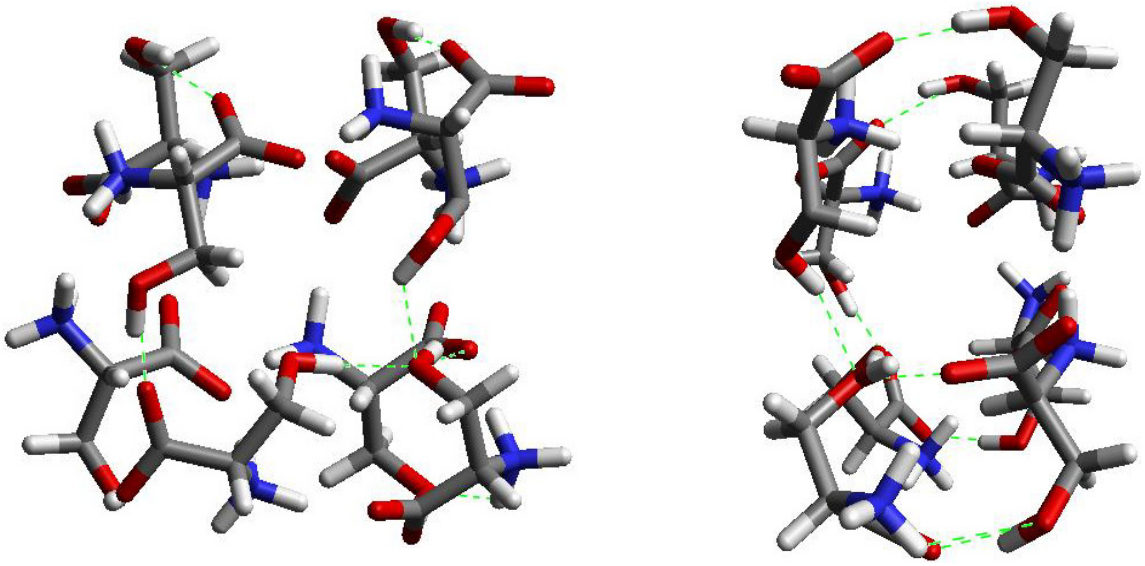

4.5

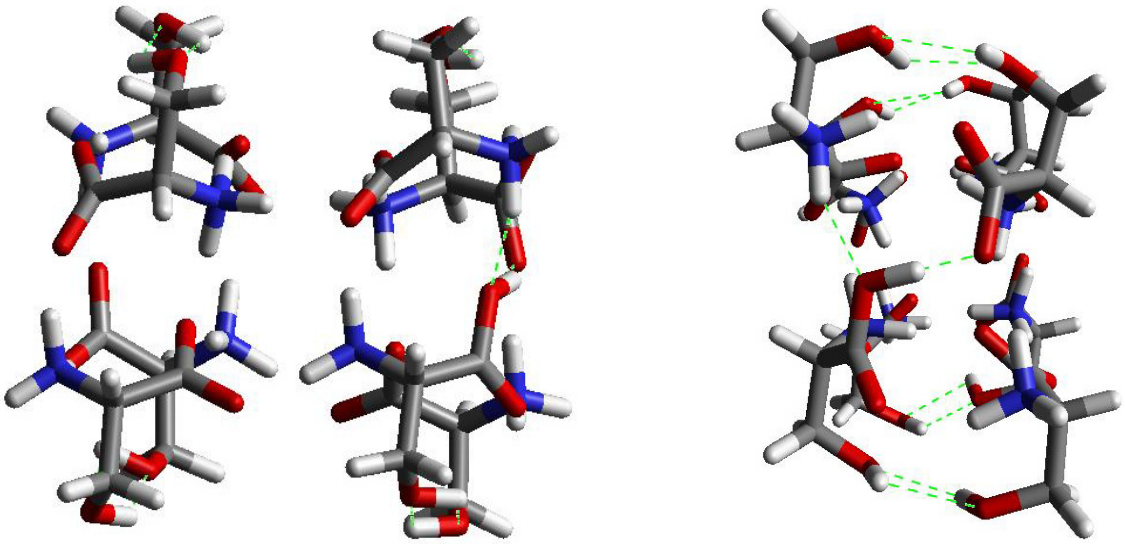

4.6

Reorganization of structure **4.5** in the gas phase leads to structure **4.6**.[18] The minimized gas phase protonated structure of **4.6** is shown, but it is virtually identical to the neutral structure. All eight serines are bound via a central zwitterionic core. The resulting cubic structure is further stabilized by hydrogen bonding between facing pairs of serines. The computed cross section for **6**, 189 $Å^2$, is in excellent agreement with the

experimental value of 187 Å^2 (Table 4.2). The gas phase binding energy of this structure is the best of any of the candidates that we have tested (Table 4.2). Given that the zwitterionic core of structure **4.6** would be essentially buried from any solvent, it has the worst solution phase binding energy of the three structures. Furthermore, a 4D/4L cluster can be assembled with a zwitterionic core and binding energy similar to that for structure **4.6**. For these reasons, **4.6** is not likely to be the solution phase structure for the serine octamer. However, **4.6** represents the most likely gas phase structure, particularly in light of the excellent gas phase energy and agreement with the experimental cross section.

Of the experimental constraints noted above for the structure of the serine octamer, (2) and (3) are the most difficult to simultaneously satisfy. A three-point interaction between each serine and the rest of the cluster would constitute the minimal requirement for chiral recognition.[28,29] It is easy to generate a variety of clusters that satisfy this requirement, but such clusters do not necessarily satisfy requirement (2). Given that eight serines must be arranged in an unusually stable structure with a cross section of 187 Å^2, cubic motifs (such as **4.5** and **4.6**) seem the most consistent with the ion mobility data. However, the symmetry of a cube generates additional problems that must be taken into account. For example, a cubic octamer connected at four points through the neutral carboxylic acids (a structure actually proposed in a concurrent work by Cooks and coworkers[30] during the preparation of this manuscript) can be assembled from homochiral serine or from 4D and 4L serines. Although each serine is held in a three-point interaction in both clusters and the energetics are nearly identical, requirement (2) is clearly not satisfied by such a structure. Furthermore the data presented in Figure 4.4 clearly demonstrates the extremely low abundance of 4D/4L clusters. In fact, it is entirely likely that all cubic

structures (the only reasonable geometry that satisfies the experimental cross section) will have an accompanying 4D/4L cluster.

The combination of requirements (2) and (3) suggests that a non-cubic structure, such as **4.4**, exists in solution which becomes cubic in the gas phase. This is depicted in cartoon fashion in Scheme 4.1. In general terms, **A** depicts various non-cubic nanocrystals of serine forming in bulk solution. In **B**, a charged serine octamer is driven to the surface of a highly charged droplet (other charges not shown for clarity). In **C** and **D**, as the number of solvent molecules is reduced (either through ion evaporation or evaporation of the solvent), the octamer begins to collapse on itself. The fully desolvated protonated serine octamer with a cubic structure is shown in **E**. In this manner the requirements for homochirality and a cubic structure can be satisfied simultaneously.

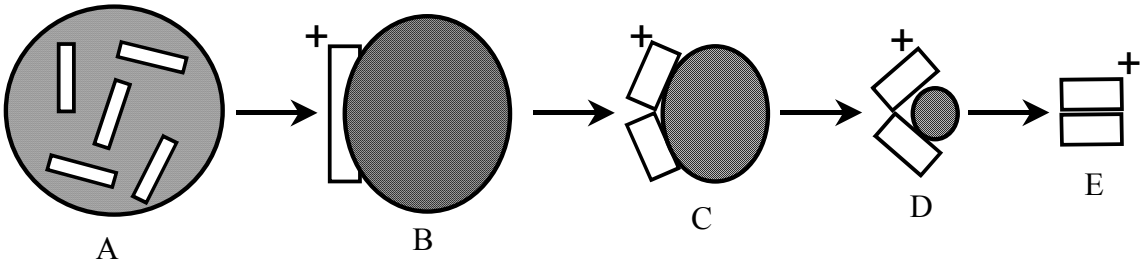

Scheme 4.1

Singly protonated structures similar to **4.4** (i.e., 6mers and 10mers) may also form in solution, however their individual transfer to the gas phase is not as favorable because only the octamer can form a cube. Aggregation of these singly charged species into multiply charged multimers (such as the multimers of the octamer shown in Figure 4.2) allows for enhanced stabilization in the gas phase. Thus larger, multiply charged clusters such as those shown in Figure 4.1 and Figure 4.3 are also present in the gas phase. However, the stability of these multimers is derived from their size, not from their

structure. Of the *singly* charged species the octamer is king. In the case of the octamer, the unusual abundance is attributed to the special stability of the cubic structure.

Both homoserine and threonine can form structures analogous to **4.4**. The crystal structure of homoserine allows for a homoserine analog of **4.4** with very little rearrangement.[31] However, in the case of threonine, substantial rearrangement from the crystal structure is necessary.[32] This may account for the reduced relative abundance of the octamer for threonine (Figure 4.8). Notwithstanding, the facile incorporation of threonine into the octamer as shown in Figure 4.9b and Figure 4.9c is compatible with the solution phase structure given in **4.4** and the gas phase structure shown **4.6**. It is anticipated that the clusters producing the spectra for homoserine and perhaps threonine are largely analogous to the structures that lead to the serine spectrum. The somewhat higher proton affinity of threonine and homoserine may be related to the observation that the cluster distributions of the analogs sometimes exhibit higher charge states than those observed for serine itself.

4.5 Conclusion

We have conducted a number of experiments designed to elucidate the structure of the serine octamer, and explain its abundance in electrospray ionization mass spectrometry. The octamer demonstrates a strong preference for homochirality. Experiments using L-serine methyl ester and L-N-tertbutoxycarbonyl-serine (L-tboc serine) show no cluster formation, indicating the amino and carboxylate functionalities are necessary for formation of the cluster. Ion mobility data indicates the cross section of the octamer to be 187 $Å^2$ (±2%). DFT calculations and the experimental data lead to a structure that is

derived from solution aggregates that precede formation of crystalline serine (Structure **4.4**). Structure **4.4** provides the necessary enantiomeric discrimination observed in the serine octamer and the folding of **4.4** into **4.5**, which relaxes to **4.6**, enables the octamer to conform to the measured cross-section with an energetically favored structure. Both threonine and homoserine may form structures analogous to the serine octamer. Threonine may incorporate freely into serine clusters because the additional methyl group does not interfere with the bonding of the cluster.

The combination of the solution and gas phase properties of the serine octamer leads to its unusual abundance when sampled by mass spectrometry. We have taken advantage of this unusual abundance to demonstrate clearly that small molecular clusters can demonstrate a preference for homochirality. This offers a molecular cluster parallel to the macroscopic observation of chiral symmetry breaking through crystal formation, and a possible pathway for the establishment of prebiotic homochirality. In appropriate energetic or chemical environments, covalent coupling of the components of the clusters could occur, creating homochiral polymers or macromolecules with well-defined stereochemistry. Such stereoregular molecules could then serve as templates in reproductive chemical systems. No inherent preference is given to a particular enantiomer in the formation of these clusters, and therefore an additional mechanism would be required to explain the eventual elimination of one enantiomer.

On a different note, ESI may offer a new experimental technique for investigating the early stages of homogeneous crystal nucleation in solution. A universal theory for the explanation of homogeneous nucleation is still lacking.[33] Several spectroscopic methods have been employed to study crystal nucleation,[34] but mass spectrometry offers the

additional ability to sample small clusters and study them in the gas phase. As appears to be the case in the present study, the solution phase structures of the clusters may not be retained in the gas phase. The difference between the solution and gas phase cluster distributions will depend on the detailed mechanism by which they are transferred from solution to the gas phase in the ESI process. The ESI process may increase the monomer concentration through evaporation prior to droplet fissioning. This could conceivably induce greater cluster formation in a super saturated and cooled droplet. If ESI does enhance the formation of nanocrystals, then one could conceivably devise a crystal-seeding source designed to initiate crystallization.

4.6 References

[1] (a) Podlech, J. Cell. Mol. Life Sci. **2001**, 58, 44-60. (b) Editor, David B. Cline *Physical origin of homochirality in life : Santa Monica, California, February 1995* Woodbury, New York : American Institute of Physics, 1996.

[2] (a) Avalos, M. A.; Babiano, R.; Cintas, P.; Jimenez, J. L.; Palacios, J. C. *Chem. Commun*. **2000**, *11*, 887-892. (b) Soloshonok, V. A.; Svedas, V. K.; Kukhar, V. P.; Galaev, I. Yu.; Kozlova, E. V.; Svistunova, N. Yu. *Bioorg. Khim*, **1993**, *19(4)*, 478-483.

[3] Buschmann, H.; Thede, R.; Heller, D. *Angew. Chem. Int. Ed*. **2000**, *39(22)*, 4033-4036.

[4] Enantiomers, Racemates, and Resolutions, Jacques, J., Wiley: New York, 1981, 217-434.

[5] Julian, R. R.; Hodyss, R.; Beauchamp, J. L. *J. Am. Chem. Soc.* **2001,** *123*, 3577-3583.

[6] Julian, R. R.; Beauchamp, J. L. *Int. J. Mass Spectrom.* **2001**, *210*, 613-623.

[7] Schalley, C. A. *Int J. Mass Spectrom*. , **2000**, *194*, 11-39.

[8] Hao, C. Y.; March, R. E.; Croley, T. R.; Smith, J. C.; Rafferty, S. P. *J. Mass Spectrom*. **2001**, *36*, 79-96.

[9] Vekey, K.; Czira, G. *Anal. Chem*. **1997**, *69*, 1700-1705.

[10] Yao, Z.-P.; Wan, T. S.; Kwong, K. -P.; Che, C. T. *Chem Comm*. **1999**, 2119-2120.

[11]Nikolaev EN, Denisov EV, Rakov VS, Futrell JH *Int J. Mass Spectrom.* **1999***,183,* 357-368.

[12] Tao, A. T.; Zhang, D.; Wang, F.; Thomas, P. D.; Cooks, R. G. *Anal. Chem*. **1999**, *71*, 4427-4429.

[13] (a) Sawada, M.; Takai, Y.; Yamada, H.; Nishida, J.; Kaneda, T.; Arakawa, R.; Okamoto, M.; Hirose, K.; Tanaka, T.; Naemura, K. J. *Chem. Soc. Perkin Trans*. *2* **1998**,

701-710. (b) Sawada, M.; Takai, Y.; Yamada, H.; Hirayama, S.; Kaneda, T.; Tanaka, T.; Kamada, K.; Mizooku, T.; Takeuchi, S.; Ueno, K.; Hirose, K.; Tobe, Y.; Naemura, K. *J. Am. Chem. Soc.* **1995**, *117*, 7726-7736. (c) Sawada, M.; Takai, Y.; Yamada, H.; Kaneda, T.; Kamada, K.; Mizooku, T.; Hirose, K.; Tobe, Y.; Naemura, K. *Chem. Commun*. **1994**, 2497-2498.

[14] (a) So, M. P.; Wan, T. S. M.; Chan, T.-W. D. *Rapid Commun. Mass Spectrom*. **2000**, *14*, 692-695. (b) Ramirez, J.; He, F.; Lebrilla, C. B *J. Am. Chem. Soc*. **1998**, *120*, 7387-7388.

[15] Sawada, M.; Shizuma, M.; Takai, Y.; Adachi, H.; Takeda, T.; Uchiyama, T. *Chem. Commun*. **1998**, 1453-1454.

[16] Krishna, P.; Prabhakar, S.; Manoharan, M.; Jemmis, E. D.; Vairamani, M. *Chem. Commun*. **1999**, 1215-1216.

[17] Clemmer, D. E.; Jarrold, M. F. *J. Mass Spectrom*. **1997**, *32*, 577-592.

[18] Hodyss, R.; Julian, R. R.; and Beauchamp, J. L. *Chirality* **2001**, *13*, 703-706.

[19] Cooks, R.G. et al. Clustering of amino acids in the gas phase by electrospray ionization mass spectrometry. Proceedings of the 48th ASMS conference on mass spectrometry and allied topics. **2000**, p.1361-1362.

[20] Mesleh, M. F.; Hunter, J. M.; Shvartsburg, A. A.; Schatz, G. C.; Jarrold, M. F. *J. Phys. Chem. A* **1996**, *100*, 16082-16086.

[21] Dugourd, P.; Hudgins, R. R.; Clemmer, D. E.; Jarrold, M. F. *Rev. Sci. Instrum.* **1997**, 68, 1122-1129.

[22] Mason, E. A.; McDaniel, E. W. *Transport Properties of Ions in Gases*; Wiley: New York, 1988.

[23] Weis, P.; Kemper, P. R.; Bowers, M. T. *J. Phys. Chem. A* **1997**, *101*, 8207-8213.

[24] Counterman, A.E.; Valentine S. J.; Srebalus, C. A.; Henderson, S. C.; Hoaglund, C. S.; Clemmer, D. E. *J. Am. Soc. Mass Spectrom.* **1998**, *9*, 743-759.

[25] Counterman, A. E.; Clemmer, D. E. *J. Phys. Chem. B* **2001**, *105*, 3646.

[26] Kistenmacher, T. J.; Rand, G. A.; Marsh, R. E. *Acta Cryst.* **1974**, *B30*, 2573-2578.

[27] (a) Jockusch, R. A.; William, P. D.; Williams, E. R. *J. Phys.Chem. A* **1999,** *103*, 9266-9274. (b) Cerda, B. A.; Wesdemiotis, C. *Analyst* **2000,***125(4)*, 657-660. (c) Jockusch, R. A.; William, P. D.; Williams, E. R. *J. Am. Chem. Soc.* **1997,** *119*, 11988. (d) Wyttenbach, T.; Witt, M.; Bowers, M. T. *Int. J. Mass Spec.* **1999,** *182/183*, 243.

[28] Tao W.A.; Zhang D. X.; Nikolaev E. N.; and Cooks R. G. *J. Am. Chem. Soc.* **2000**, *122*, 10598-10609.

[29] Ahn, S.; Ramirez, J.; Grigorean, G.; Lebrilla, C. B. *J. Am. Soc. Mass Spectrom.* **2001**, *12*, 278-287.

[30] Cooks, R. G.; Zhang, D.; Koch, K. J.; Gozzo, F. C.; Eberlin, M. N. *Anal. Chem.* **2001**, *73*, 3646-3655.

[31] Chacko, K. K.; Swaminathan, S.; Veena, K. R. *Crys. Struct. Commun*. **1982**, *11*, 2057.

[32] Janczak, J.; Zobel, D.; Luger, P. *Acta Cryst. Sec. C*. **1997**, *53*, 1901.

[33] Granasy, L.; Igloi, F. *J. Chem. Phys*. **1997,** *107*, 3634-3644.

[34] (a) Granasy, L.; James, P. F. *J. Chem. Phys*. **2000,** *113,* 9810-9821, (b) Peng, X.; Wickham, J.; Alivisatos, A. P. *J. Am. Chem. Soc.* **1998**, *120*, 5343-5344.